

RESEARCH ARTICLE



Influence of Zika virus 3'-end sequence and nonstructural protein evolution on the viral replication competence and virulence

Hae-Gwang Jung^a, Hee Cho^a, Minwoo Kim^a, Haewon Jung^a, Yeonju Bak^a, Se-Young Lee^a, Han Young Seo^a, Yu-Min Son^a, Hawon Woo^a, Gone Yoon^a, Seong-Jun Kim^{ib} and Jong-Won Oh^{ib}

^aDepartment of Biotechnology, Yonsei University, Seoul, South Korea; ^bCenter for Convergent Research of Emerging Virus Infection, Korea Research Institute of Chemical Technology, Daejeon, South Korea

ABSTRACT

Zika virus (ZIKV) has been circulating in human networks over 70 years since its first appearance in Africa, yet little is known about whether the viral 3'-terminal sequence and nonstructural (NS) protein diverged genetically from ancient ZIKV have different effects on viral replication and virulence in currently prevailing Asian lineage ZIKV. Here we show, by a reverse genetics approach using an infectious cDNA clone for a consensus sequence (Con1) of ZIKV, which represents Asian ZIKV strains, and another clone derived from the MR766 strain isolated in Uganda, Africa in 1947, that the 3'-end sequence -UUUCU-3' homogeneously present in MR766 genome and the -GUCU-3' sequence strictly conserved in Asian ZIKV isolates are functionally equivalent in viral replication and gene expression. By gene swapping experiments using the two infectious cDNA clones, we show that the NS1-5 proteins of MR766 enhance replication competence of ZIKV Con1. The Con1, which was less virulent than MR766, acquired severe bilateral hindlimb paralysis when its NS1-5 genes were replaced by the counterparts of MR766 in type I interferon receptor (IFNAR1)-deficient A129 mice. Moreover, MR766 NS5 RNA-dependent RNA polymerase (RdRp) alone also rendered the Con1 virulent, despite there being no difference in RdRp activity between MR766 and Con1 NS5 proteins. By contrast, the Con1 derivatives expressing MR766 Nsps, like Con1, did not develop severe disease in wild-type mice treated with an IFNAR1 blocking antibody. Together, our findings uncover an unprecedented role for ZIKV NS proteins in determining viral pathogenicity in immunocompromised hosts.

ARTICLE HISTORY Received 4 May 2022; Revised 12 September 2022; Accepted 20 September 2022

KEYWORDS Zika virus; infectious cDNA clone; virulence determinant; 3'-end sequence variants; nonstructural proteins

Introduction


Zika virus (ZIKV) has emerged as a global health security threat since the recent outbreaks in Brazil and the Americas from 2015 to 2016. ZIKV infection can cause not only rash, fever, dizziness, anorexia, and arthralgia but also various severe neurological disorders including microcephaly in infants and Guillain-Barré syndrome, meningoencephalitis, and myelitis in adults [1,2].

ZIKV was first discovered from rhesus monkey in the Zika forest of Uganda in 1947 (MR766/Uganda/1947; NC_012532.1) [3]. After the first confirmed human infection reported in Uganda in 1962 [4-6], ZIKV was isolated from *Aedes aegypti* mosquitoes in Malaysia in 1966 (P6-740/Malaysia/1966; HQ234499.1) [7,8], which was the first case of ZIKV detection in Asia. The first human case was then reported in Central Java Indonesia by the diagnosis of seroconversion [9]. Following less than 20 sporadic cases of ZIKV infection in African and Southeast Asian countries [10], a

significant outbreak of ZIKV infection began in 2007 on Yap Island (Yap/Micronesia/2007; EU545988.1), Micronesia, affecting ~73% of the Yap residents [11]. In 2013-2014, ZIKV spread to French Polynesia, infected about 11% of the population, and caused large epidemics in the South Pacific regions [12,13]. Most recently, a large epidemic occurred in Brazil in May 2015 when there was a marked increase in microcephaly cases reported among newborn infants [14]. Over the last 7 decades, ZIKV has been crossing host barriers to invade humans, generating two phylogenetically distinct lineages, namely African and Asian lineages [15].

ZIKV has a single-stranded positive sense RNA genome of about 10.8 kb in length. The viral genome consists of 5'-untranslated region (UTR), a single open reading frame (ORF), and 3'-UTR. The ORF encodes a single polyprotein that is processed by viral and host proteases into three structural proteins (capsid, pre-membrane/membrane, and envelope) and seven nonstructural proteins (Nsps including

CONTACT Jong-Won Oh  jwoh@yonsei.ac.kr  Department of Biotechnology, Yonsei University, 50 Yonsei-ro, Seodaemun-gu, Seoul 03722, South Korea

 Supplemental data for this article can be accessed online at <https://doi.org/10.1080/22221751.2022.2128433>.

© 2022 The Author(s). Published by Informa UK Limited, trading as Taylor & Francis Group, on behalf of Shanghai Shangyixun Cultural Communication Co., Ltd. This is an Open Access article distributed under the terms of the Creative Commons Attribution-NonCommercial License (<http://creativecommons.org/licenses/by-nc/4.0/>), which permits unrestricted non-commercial use, distribution, and reproduction in any medium, provided the original work is properly cited.

NS1, NS2A, NS2B, NS3, NS4A, NS4B, and NS5), which are involved in viral genome replication and evasion of host antiviral immune responses. Among the Nsps, NS5 with RNA-dependent RNA polymerase (RdRp) activity is the key enzyme required for viral replication [16,17]. ZIKV has been undergoing significant evolutionary changes since it was first discovered in Uganda [18]. In both UTRs and a single ORF of ZIKV genome, there are substantial sequence variations between the African and Asian lineage ZIKVs. Evolution through gradual or step-gradient changes in viral genome is inevitably associated with altered viral phenotypes such as growth and virulence, enabling a virus to adapt to a new host and evade its immune responses. It is still largely unknown to what extent genetic differences between the two distinct ZIKV lineages affect disease severity in human [19].

The clinical symptoms observed in patient with an early discovered African lineage ZIKV is limited. However, the disease severity observed during recent ZIKV outbreak in Brazil in 2015 points that, although infected patients still develop various real-world clinical outcomes such as encephalitis etc., ZIKV appears to become less pathogenic and lethal *in vitro* and in both type-I interferon receptor knockout (A129) mice and immunocompetent mice. Furthermore, brain tropism of ZIKV was more evident for African lineage ZIKV [6,20–22].

Viral pathogenicity is determined by viral genome replication competence and thereby viral gene products. ZIKV structural proteins have been considered to be major determinants of viral pathogenicity [23–25]. Considering their essential roles in viral replication and gene expression, non-coding *cis*-acting RNA elements in the viral genome can also play a role in the determination of ZIKV pathogenicity. The 3'-end of ZIKV and other flaviviruses terminates with a conserved CU_{OH} instead of a poly(A) tract. The 3'-terminal dinucleotide CU_{OH} functions as the recognition site for the dengue virus RdRp [26,27]. While this dinucleotide is highly conserved in flaviviruses, there are evolutionally diverged sequences 2-nt upstream of this *cis*-acting RNA element in ZIKV genome. Asian/American lineage ZIKV strains have the -GUCU-3' sequence diverged from the -UUUCU-3' sequence found in the prototype African lineage ZIKV strain MR766. Currently, little is known about the impact of this 3'-end sequence change during the course of ZIKV evolution.

In this study, we investigated whether the ZIKV lineage-specific 3'-end sequences and Nsps play critical roles in determining viral replication capability and pathogenicity, using a reverse genetics approach using infectious cDNA clones derived from the African ZIKV strain MR766 and a consensus genome

sequence (Con1) of ZIKV, which represents an Asian lineage ZIKV. Our results provide evidence that the two 3'-terminal sequences, -GUCU-3' and -UUUCU-3' are functionally compatible with both African and Asian lineages of ZIKV and that ZIKV Nsps are virulence determinants associated with African lineage ZIKV neurovirulence in interferon (IFN) α/β receptor knockout (IFNAR^{-/-}) mice and wild-type (WT) C57BL/6 mice transiently blocked in type I IFN signaling.

Materials and methods

Cell culture and virus infection

Human hepatocellular carcinoma Huh7, human alveolar epithelial A549 (CCL 185), and African green monkey kidney-derived Vero E6 (CRL 1586) cells were cultivated in Dulbecco's modified Eagle's medium (DMEM) supplemented with 10% fetal bovine serum (FBS), 100 U/ml of penicillin and 100 μ g/ml streptomycin at 37°C in 5% CO₂. Similarly, *Aedes albopictus* C6/36 mosquito cells (CRL 1660) were also cultivated in complete DMEM at 28 °C in 5% CO₂. All cell lines were obtained from the American Type Culture Collection (ATCC, Rockville, MD, USA). The ZIKV MR766 (ATCC VR-84) and PRVABC59 (ATCC VR-1843) strains with unknown passage history were obtained from the ATCC. After titering these stocks, passage 2 (P2) virus stocks for MR766 and PRVABC59 were prepared and used in infection experiments and RNA sequencing. ZIKV was propagated in Vero E6 cells grown in DMEM containing 2% FBS. Unless otherwise specified, cells were seeded in a 10-cm dish, cultured overnight, and then infected with viruses at an MOI of 0.1 or 0.01 by incubating at 37 °C for 2 h. After washing, the infected cells were maintained in a complete medium supplemented with 10% FBS for the indicated periods as specified in figure legends.

Construction of full-length cDNA clones of ZIKV

A full-length cDNA clone for a consensus sequence of ZIKV (Con1) was initially constructed in a low-copy number plasmid pMW119 (Nippon Gene, Tokyo, Japan). Three chemically synthesized cDNA fragments, Con1-1, Con1-2, and Con1-3, which represent ZIKV genome nucleotides (nt) 37–3,445, 3,426–5,870, and 5,851–8,430, respectively, (according to nt number of Con1 strain; GenBank accession number ON123673), and the synthetic DNA Con1-B were obtained from Bioneer (Daejeon, South Korea). The Con1-B is composed of a T7 promoter; 51-nt 5'-end region of ZIKV genome; a multiple cloning site (MCS) containing NheI, ApaLI, KasI, and SfiI sites; 2,392-nt 3'-region sequences (nt 8,416–10,806) of

viral genome; and a reverse-oriented EciI site fused to the 3'-end of a 11-nt random sequence (designed to generate authentic 3'-end viral genome sequence following run-off transcription of an EciI-linearized full-length cDNA clone). The cassette vector pMW119-Con1-5'-3' was generated by assembling PCR-amplified Con1-B cDNA fragment and HindIII/SmaI-digested pMW119, using In-Fusion HD cloning kit (Takara Bio, Tokyo, Japan). Then the three cDNA fragments, Con1-1 to Con1-3 were digested with selected restriction enzymes, gel-purified, and sequentially cloned into the MCS of pMW119-Con1-5'-3' to generate a full-length cDNA clone, termed pMW-T7-ZK-Con1. The primers used to generate pMW-T7-ZK-Con1 infectious cDNA clone are presented in Supplementary Table S1.

The full-length Con1 cDNA was subcloned into a pBeloBAC11 vector derivative, pBAC-T7-HDVr containing a T7 promoter and an HDVr sequence [28] followed by SacII site. The pBAC-T7-HDVr vector was generated by insertion of a T7 promoter-tagged HDVr gene into the pBAC-Vec cassette derived from pSARS-REP-Feo [29]. The full-length cDNA clone of Con1 was PCR-amplified using Herculase II Fusion DNA polymerase (Agilent technologies, Santa Clara, CA, USA) and then subcloned into a linear pBAC-T7-HDVr cassette using In-Fusion HD cloning kit (Takara Bio) to generate pBAC-T7-ZK-Con1. The primers used to generate pBAC-T7-ZK-Con1 infectious cDNA clone are presented in Supplementary Table S2.

Similarly, a full-length cDNA clone of ZIKV Uganda strain MR766 was constructed by assembling cDNA into a linear form of pBAC-T7-HDVr cassette vector generated by inverse-PCR using pBAC-T7-HDVr as a backbone and the primers pBAC-T7-HDVr_F (forward primer) and pBAC-T7-HDVr_R (reverse primer). The total RNA used for cDNA synthesis was extracted from a culture adapted MR766 (passaged four times in Vero E6 cells after receiving ATCC VR-84 viral stock) using TRIzol LS reagent (Invitrogen, Carlsbad, CA, USA). Three cDNA fragments synthesized using SuperScript III First-Strand Synthesis System (Invitrogen) were used to construct a full-length clone of MR766 (GenBank ON123672). The primers used to generate pBAC-T7-ZK-MR766 infectious cDNA clone are presented in Supplementary Table S3.

The full-length ZIKV cDNA clones with 3'-end sequence variations or with a heterologous NS5 or NS1-5 genes were generated using In-Fusion HD cloning kit (Takara Bio). The primers used to generate derivatives of Con1 and MR766 cDNA clones bearing heterologous 3'-end sequences are presented in Supplementary Tables S2 and S3.

All works using ZIKV genes were approved by the Institutional Biosafety Committee (IBC) at Yonsei

University (IBC-A-202106-282-03, June 25, 2021 and IBC-A-202103-270-02, 2 March 2021). The genetic integrity of all the cDNA clones constructed in the present study was confirmed by sequencing analysis.

Construction of a ZIKV subgenomic replicon expressing *Renilla luciferase*

To construct CMV promoter-based ZIKV subgenomic replicon (sgRep), initially the CMV-ZK-Con1-HDVr cDNA fragments amplified from pBAC-T7-ZK-Con1 and pBAC-T7-ZK-Con1(TTTCT) were cloned into a linear pBAC-CMV-5'-3' cassette to produce pBAC-CMV-ZK-Con1 and its derivative pBAC-CMV-ZK-Con1(TTTCT) using In-Fusion HD Cloning Kit (Takara Bio). A *Renilla luciferase* (Rluc) gene fused to puromycin resistance gene (Puro), Puro-2A-Rluc-2A, in which Rluc and Puro genes were fused to FMDV 2A sequence for self-processing, was generated by two sequential bridging PCRs. The reporter-coding gene was cloned into the linear sgRep cassettes using In-Fusion HD Cloning Kit (Takara Bio) to generate ZIKV sgReps [pBAC-CMV-ZK-Con1_sgRep, pBAC-CMV-ZK-Con1_sgRep(TTTCT), and pBAC-CMV-ZK-Con1_sgRep(NS5_GAA)]. Primers used to generate pBAC-CMV-ZIKV-Con1 and its derivatives, including ZIKV subgenomic replicons, are listed in Supplementary Table S4.

Plasmids and reagents

The Rluc gene flanked by ZIKV 5'-UTR and 3'-UTR (terminating with -GTCT-3' or -TTTCT-3') was fused to the T7 promoter and inserted into pcDNA3.1 plasmid to produce an Rluc-expressing Con1-derived minigenome terminating with -GTCT-3' [Con1-minigenome(GUCU)-Rluc] or -TTTCT-3' [Con1-minigenome(UUUCU)-Rluc], which was used to test the effect of ZIKV 3'-end sequence variances on viral gene expression. To express NS5 proteins of ZIKV MR766 and Con1 in *E. coli*, pTrcHisB-ZK-MR766_NS5 and pTrcHisB-ZK-Con1_NS5 plasmids were constructed by inserting the corresponding NS5-coding cDNAs, which were amplified by RT-PCR using two NS5-specific primer sets (MR766_NS5 forward primer 5'-GCTAGCGGAGGTGGGACGGGAGAG-3' and reverse primer 5'-GAATTCTTACAACACTCCGGGTGTGGAC-3' or Con1_NS5 forward primer 5'-GCTAGCGGGGTTGGAACAGGAGAG-3' and reverse primer 5'-GAATTCTTACAGCACTCCAGGTGTAGACC-3') and MR766 (P2) viral RNA or pMW-T7-ZK-Con1 as a template, into the NheI and EcoRI sites of pTrcHisB vector (Invitrogen).

For the generation of a mammalian vector expressing ZIKV pre-membrane and envelope protein (prME, aa 123-794) fused to the membrane-anchored Capsid (Capsid anchor, Ca; aa 105-122), CaprME-encoding gene was

PCR-amplified from infectious cDNA clones for Con1 and MR766 ZIKVs using two different strain-specific primer sets (MR766 CaprME, forward primer 5'-TTTAAAC TTAAGCTTGCCACCATGGGCGCAGACACCAGCA TCG-3' and reverse primer 5'-ATATCTGCAGAATTC TTAATCA AGCAGAAACAGCCGTGGAGAGG-3'; Con1 CaprME, forward primer 5'-TTTAAACTTAAGC TTGCCACCATGGGCGCAGATACTAGTGTCTGGA-3' and reverse primer 5'-ATATCTGCAGAATTC TTAATCA TCAAGCAGAGACGGCTGTGGATAAG-3'). pUMVC (# 8449) and pBABE-puro (# 1764) plasmids used to generate murine leukaemia virus (MLV)-based pseudotype virus loaded with ZIKV prME were obtained from Addgene (Addgene, Watertown, MA, USA).

The nucleoside analogue 2'-C-methyladenosine (2'-CMA) [30] was obtained from Cayman Chemical (Ann Arbor, MI, USA). A murine monoclonal antibody (MAb) preventing type I IFN signaling MAb-5A3 was purchased from Leinco Technologies (St. Louis, MO, USA).

In vitro RNA transcription

For preparation of ZIKV RNA by *in vitro* transcription (IVT), ZIKV infectious cDNA clone was linearized with SacII restriction enzyme. Following phenol-chloroform extraction, the linearized DNA was transcribed *in vitro* using a T7 mMESSAGE mMACHINE kit (Ambion, Austin, Texas, USA). After removal of DNA template by DNase I treatment, viral RNA transcript was extracted with phenol-chloroform.

To obtain a full-length (FL) 3'-UTR (428 or 429 nt) and the 3'-terminal stem-loop (SL) RNA (3'-SL, 82 or 83 nt) that were used in an *in vitro* RNA decay assay, DNA templates were generated using pBAC-T7-ZK-Con1 and its derivative pBAC-T7-ZK-Con1(TTTCT) as templates by PCR using a forward primer containing the T7 promoter sequence (underlined) 5'-TAA-TACGACTCACTATAGCACCAATCTTAATGTTGTCAGG-3' (for FL 3'-UTR) or 5'-TAATACGACTCACTATAGACTCCATGAGTTTCCACCAC-3' (for 3'-SL) and a reverse primer containing the sequence complementary to -GTCT-3' or -TTTCT-3', 5'-AGACCCATGGATTTCCCCAC-3' (ZK-Con1_R; the sequence complementary to the 3' terminal sequence is underlined) or 5'-AGAAACCATGGATTTCCCCAC-3' (ZK-Con1_R(TTTCT)). The templates for ZIKV-derived subgenomic flavivirus RNAs [sfRNA1 (412 nt) and sfRNA2 (328 nt)], which were used as size markers, were PCR-amplified from pBAC-T7-ZK-Con1 using a set of primers specific to the sfRNA start site (T7_sfRNA1_forward primer 5'-TAATACGACTCACTATAGTGTCTCAGGCCTGCTAGTCAGCCACAG-3' or T7_sfRNA2_forward primer 5'-TAATACGACTCACTATAGGTCAGGCCGAGAACGCCATGGCAC-3'; the G in italic is an extra

sequence added for efficient IVT) and the same reverse primers used to generate the template for the FL 3'-UTR. The resulting PCR products were resolved by electrophoresis on a 2% agarose gel, purified using HiYield Gel/PCR DNA Mini Kit (Real Biotech Corp., Taipei, Taiwan), and used for *in vitro* transcription using T7 MEGascript kit (Ambion). A mixture of rNTPs including 0.15 μ M rGTP, 10 μ Ci [α - 32 P] of rGTP (3,000 Ci/mmol, Amersham Pharmacia Biotech) was used for radioisotope labelling of FL 3'-UTR and 3'-SL.

Rescue of recombinant viruses from infectious cDNA clones

Recombinant ZIKVs were rescued from infectious cDNA clones, as previously described [31]. Briefly, 2.2×10^6 Vero E6 cells seeded on a 10-cm dish were grown overnight and transfected with 10 μ g of *in vitro* transcripts of viral genome using Lipofectamine 2000 (Invitrogen). After incubation for 4 h, cells were washed twice with PBS and cultured in fresh media containing 2% FBS, 100 U/ml of penicillin and 100 μ g/ml streptomycin until clear signs of cytopathic effects (CPE) were seen. Approximately 3–5 days after transfection, culture supernatant was harvested by clearing cell debris by centrifugation to obtain P0 (passage 0) viral stock for further analyses. The first passage (P1) from Vero E6 cells was used for infection experiments.

Plaque assay

Viral titre was determined by plaque-forming assay as previously reported [32]. Briefly, Vero cells were seeded in a 6-well plate, cultured overnight, and infected with 10-fold serially diluted virus samples in a serum-free medium for 1 h. After washing with PBS, cells were overlaid with DMEM containing 1% low-melting agarose (Sigma-Aldrich, St. Louis, MO, USA), 2% FBS, 100 U/ml of penicillin, and 100 μ g/ml streptomycin. After incubation for 3–4 days until clear plaques were observed, cells were fixed with 10% formaldehyde and stained with 1% crystal violet solution.

Real-time reverse-transcription quantitative PCR (RT-qPCR)

Total RNA was extracted using TRIzol Reagent (Invitrogen). ZIKV genomic RNA copy number was determined as previously described [33] with minor modifications. Briefly, 1 μ g of total RNA was subjected to cDNA synthesis using ImProm-II reverse transcriptase (Promega, Madison, WI, USA). Real-time RT-qPCR was carried out using TOPreal qPCR 2X Pre-MIX (SYBR Green with low ROX) (Enzynomics,

Daejeon, South Korea) and a set of primers [a forward primer gRNA-3478F (5'-GTATGGAATGGAGA-TAAGGCCCA-3') and a reverse primer gRNA-3669R (5'-GCACATCAATGGCAGTGTGGT-3')] [34] on a Bio-Rad CFX real-time PCR detection system (Bio-Rad). Standard RNA was prepared by *in vitro* transcription using a T7 promoter-fused DNA template representing nt 3442–3701 of ZIKV NS1-NS2A gene.

Immunoblotting

Virus-infected cells were resuspended in a lysis buffer [50 mM Tris-HCl (pH 8.0), 150 mM NaCl, and 1% NP-40] supplemented with an EDTA-free protease inhibitor cocktail (Roche Diagnostics, Mannheim, Germany) and incubated on ice for 20 min. After centrifugation at 12,000 × *g* for 20 min, cleared cell lysates were subjected to sodium dodecyl sulfate-polyacrylamide gel electrophoresis, followed by immunoblot analysis using an appropriate set of primary and secondary antibodies. Antibodies were obtained as follows: rabbit polyclonal anti-NS5 (Lab made; 1:1,000 dilution), rabbit polyclonal anti-NS3 (GeneTax Inc., Irvine, CA, USA; GTX133309 at 1:1,000 dilution), and rabbit polyclonal anti-Capsid antibody (GeneTax; GTX133317 at 1:1,000 dilution), and mouse monoclonal anti- α -tubulin antibody (Calbiochem, La Jolla, CA, USA; DM1A at 1:5,000 dilution). Proteins were visualized using enhanced chemiluminescence.

Luciferase assay

Transfected cells were lysed using Glo Lysis buffer (Promega). Cleared cell lysates were obtained by centrifugation at 12,000 × *g* for 20 min at 4 °C. The protein concentrations of the lysates were determined using Bradford assay and the Rluc activity was measured using Glo Luciferase assay kit (Promega) in a GloMax-Multi Detection System (Promega).

NS5 protein expression and purification

ZIKV NS5 protein was expressed in *E. coli* Rosetta cells (Sigma-Aldrich) transformed with pTrcHisB-ZK-MR766_NS5 or pTrcHisB-ZK-Con1_NS5 and purified by affinity chromatography using Ni-NTA (nickel-nitrilotriacetic acid) resin (Qiagen, Valencia, CA, USA) followed by ion-exchanger chromatography using a SP-Sepharose column (GE Healthcare Life Sciences), as described previously [17].

RdRp assay

In vitro RdRp assay was performed as described previously [35]. Briefly, 5 pmol of recombinant ZIKV NS5 in a total volume of 25 μ l reaction buffer

[50 mM Tris-HCl (pH 8.0), 50 mM NaCl, 2.5 mM MnCl₂, 1 mM DTT, 10% glycerol, and 20 units of RNase inhibitor] containing 1 μ g of poly(A) RNA template, 5 μ M complementary rUTP, 5 μ Ci [α -³²P] of rUTP (3,000 Ci/mmol, Amersham Pharmacia Biotech). The reaction mixture was incubated for 2 h at 30 °C. After the RdRp reaction, products were resolved on a denaturing 7.5% polyacrylamide gel containing 8 M urea, prior to autoradiography and quantification using a PhosphorImager.

RNA decay assay

In vitro RNA decay assay was performed as described previously [36]. Briefly, synthetic ZIKV FL 3'-UTR RNA (nt 1–428 or 1–429) or 3'-terminal SL RNA (nt 347–428 or 347–429) (10 pmol each) was incubated at 37 °C with Vero E6 (40 μ g) or C6/36 cell lysates (10 μ g) in a 130 μ l reaction buffer [50 mM Tris-HCl (pH 8.0), 150 mM NaCl, 0.1% NP-40, and 10% glycerol] supplemented with complete EDTA-free 1× protease inhibitor cocktail (Roche Diagnostics) for the times indicated in the figure legends. After the reaction, RNA was extracted from a 25- μ l aliquot of the reaction mixture and resolved on a denaturing 5 or 10% polyacrylamide gel containing 8 M urea. After electrophoresis, the gel was exposed to a PhosphorImager plate for quantification of radioactive signals.

RACE-PCR for ZIKV 3'-end sequence analysis

RNA was extracted from ZIKV (MR766 or PRVABC59) with TRIzol LS (Invitrogen) and purified according to the manufacturer's protocol. RNA was ligated to the 5'-adenylated DNA adaptor (5'-TGGAATTCTCGGGTGCCAAGG-3') using a truncated T4 RNA ligase 2, (NEB, UK) and was reverse-transcribed to cDNA using an RT primer (5'-GCCTTGGCACCCGAGAATTCCA-3'). The cDNA was amplified using a forward primer targeting 3'-UTR of viral genome (nt 10,607–10,627) (5'-CCCTTCAATCTGGGGCCTGAA-3') and the RT primer targeting the 5'-adenylated adaptor. The amplified PCR products were size-fractionated by electrophoresis on an agarose gel to recover DNA fragments and subjected to sequencing analysis on an Illumina Nextseq instrument (Illumina, San Diego, CA, USA).

Next generation sequencing

ZIKV (PRVABC59, P2) RNA was extracted from the culture supernatant of Vero E6 cells with TRIzol LS (Invitrogen) and purified according to the manufacturer's protocol. The sequencing libraries were prepared using the TruSeq Stranded Total RNA with Ribo-Zero H/M/R_Gold kit (Illumina, San Diego,

CA, USA). Libraries were sequenced using an Illumina NovaSeq platform (NovaSeq 6000 system, Macrogen Inc. South Korea) as 295-nt paired ends. The FastQC (v0.11.8) was used to check the read quality. Trimmomatic (v0.38) was used to remove adapter sequences and low quality read sequences. ZIKV RNA-seq data in fastq format were deposited in the NCBI Sequence Read Archive (SRA) under the accession number SRR20766619. After mapping filtered data to the reference genome sequence using the BWA-MEM algorithm (BWA v0.7.17) [37], duplicated reads were removed with Sambamba (v0.6.7). Genome coverage analysis, mapping ratio calculation, and variant calling were performed using SAMtools (v.1.6) and BCFtools (v.1.6). At this step, SNPs and short indels candidates with a phred score above 30 (base call accuracy of 99.9%) were captured and annotated using SnpEff (v.4.3t) to assess mutation profile.

Phylogenetic analysis

Multiple sequences of ZIKV were aligned using MUSCLE (v3.8.31). The phylogenetic tree was constructed using Molecular Evolutionary Genetics Analysis (MEGA) v11 software by the maximum likelihood method with 1,000 bootstrap replicates.

Pseudotyped virus entry assay

ZIKV prME protein-pseudotyped MLV expressing nanoluciferase was generated as previously described [35,38]. Briefly, HEK293T cells were transfected with pUMVC, pBABE-puro-NanoLuc, and a mammalian vector expressing the ZIKV CaprME. The culture supernatant harvested 2 days after transfection was centrifuged at $1500 \times g$ for 10 min and passed through 0.45 μm filter to remove cell debris. Pseudotyped MLV titre was quantified using qRT-PCR. Packaged viral RNA was extracted using TRIzol LS reagent (Invitrogen) according to the manufacturer's instructions and subjected to reverse transcription and qRT-PCR using primers targeting the 5' LTR region of MLV RNA (forward primer 5'-ATTGACTGAGTCGCCCCGG-3' and reverse primer 5'-AGCGAGACCACAAGTCGGAT-3'). To transduce HEK293T cells with the pseudotyped virus, target cells were seeded in a 12-well cell culture plate and inoculated with 0.5 ml media containing pseudotyped virus for 9 h. Cells were then washed and further cultivated in fresh complete media for 48 h prior to measuring reporter activity using a Nano-Glo Luciferase assay kit (Promega) and the Glo-Max-Multi Detection System (Promega).

Histopathological analysis

Brain tissue samples from mice were fixed in 10% formalin in PBS, paraffin-embedded, sectioned at 4 μm

thickness, stained with hematoxylin and eosin (H&E). Digital images captured were analyzed using an Aperio AT2 scanner (Leica Biosystems, Nussloch, Germany).

Animal experiments

A129 mice (seven- to eleven-week-old), which lack the type I IFN α/β -receptor, were obtained from the Woojung Bio (Suwon, South Korea). C57BL/6 mice (six-week-old) were purchased from the Jabilio (Suwon, South Korea). Mice of different genders were housed in separate cages. A129 mice ($n = 12$ per each group with 4 female and 8 male mice) infected in both hind foot pads with 10^2 plaque forming units (PFU) of recombinant ZIKV [Con1, Con1/MR_NS5, Con1/MR_NS1-5, rMR766] in 100 μl (50 μl /foot pad) of PBS. Wild-type C57BL/6 mice ($n = 10$ per each group with 5 female and 5 male mice) were infected with 10^4 PFU of recombinant ZIKV [Con1, Con1/MR_NS5, Con1/MR_NS1-5, rMR766] via ip route in a total volume of 100 μl . The C57BL/6 were injected ip with a total of 3.0 mg/kg of a monoclonal antibody 5A3 (Mab-5A3) targeting the IFNAR-1 subunit of the mouse IFN- α/β receptor [Leinco Technologies, St. Louis, MO, USA; 2.0 mg/kg first dose at -1 day post-infection (dpi) followed by two 0.5 mg/kg subsequent doses at 1 and 4 dpi] to interfere with type I IFN-induced intracellular signaling. Mice were monitored daily for clinical illness (hindlimb and forelimb paralysis) for 15 days and humanely euthanized when losing >20% of initial body weight. Blood was collected at the time points indicated in each figure by tail incision to monitor viral loads in sera or from euthanized mice via intracardiac bleeding. Following perfusion with PBS, tissues (brain, testis, kidney, liver, and spleen) were harvested, homogenized in PBS, and centrifuged to harvest supernatants. Sera were separated by centrifugation at $6,000 \times g$ for 5 min and stored at -80°C until used. Viral loads in tissues and sera were determined by RT-qPCR and plaque assay.

Ethics statement

All animal experiments were performed in accordance with the Korean Ministry of Food and Drug Safety guidelines. Experimental procedures were reviewed and approved by the Institutional Animal Care and Use Committee of the Yonsei University (IACUC-A-202108-1313-03 and IACUC-A-202207-1501-02). At the end of experiments, all mice were euthanized by CO_2 inhalation.

Statistical analysis

Statistical analysis was performed using GraphPad Prism 8 (GraphPad Prism Software Inc., La Jolla,

CA, USA). Differences in means were analyzed using a two-tailed, unpaired Student's *t*-test or one-way ANOVA, as indicated in the figure legends. The Kaplan-Meier survival curves were analyzed by the log-rank (Mantel-Cox) test. Unless otherwise specified, quantitative results were presented as mean \pm standard deviation (SD) of at least three independent experiments. A *P* value of less than 0.05 was considered statistically significant.

Results

Construction of a full-length cDNA clone for a consensus genome sequence of ZIKV

In this study, we generated an infectious cDNA clone for a ZIKV consensus sequence by inserting its cDNA fragments into a BAC vector (Figure 1A). We used 12 full-length ZIKV genome sequences, including the ones for which infectious cDNA clones were established, and 38 additional nearly complete genome sequences with complete ORF sequences of various African and Asian lineage ZIKVs (Supplementary Table S5) to retrieve a consensus, full-length genome sequence, termed Con1 (GenBank accession number ON123673). The Con1 sequence was more similar to the genome sequence of the currently isolated Asian lineage ZIKV PRVABC59 (KU501215.1) in comparison to that of the prototype African strain MR766 (AY632535.2) (98.5% vs. 93.5% in sequence identity), as can be seen in a ZIKV phylogenetic tree (Supplementary Figure S1), since the sequence sets used to generate the consensus sequence Con1 were skewed toward Asian strains for which more full-genome sequences are available. The Con1 cDNA fragments were chemically synthesized and initially joined to a cassette vector derived from a low copy number plasmid pMW119 to generate pMW-T7-ZK-Con1, from which the full-length cDNA clone was subcloned into a modified BAC vector to obtain pBAC-T7-ZK-Con1, as described in detail in Materials and methods.

Infectivity of rescued, recombinant ZIKV Con1

Rescue of recombinant ZIKV Con1 was carried out by transfecting Vero E6 cells with *in vitro* synthesized T7 transcripts generated from SacII-linearized pBAC-T7-ZK-Con1. The progeny virus (passage number 0, P0) was harvested when CPE was clearly seen (*ca.* ~3–5 days post-transfection) in the transfected cells and passaged consecutively to prepare P1 and P2 viral stocks. All of these rescued and passaged viruses produced infectious viruses as evidenced by the high viral titres (*ca.* over 10^5 PFU/ml in P1 and P2) while the Con1(NS5_GAA) with a GAA substitution at the NS5 active site, as expected, failed to generate infectious virus (Figure 1B).

Infectivity of the rescued virus (P3) was further verified in Huh7 cells, in which viral RNA levels peaked to $>10^9/\mu\text{g}$ total RNA within the infected cells and $>10^{10}/\text{ml}$ culture supernatant at 3 dpi (Supplementary Figures S2A and B). Expression of both viral nonstructural proteins (NS3 and NS5) and the capsid were confirmed by immunoblotting (Supplementary Figure S2C). Altogether, these results demonstrated the infectivity of the rescued recombinant ZIKV Con1.

Growth attenuation property of ZIKV Con1

Since ZIKV Con1 has no parental strain, we used an Asian lineage ZIKV PRVABC59 isolated in Puerto Rico in 2015 to compare their replication capability. While these two viruses only differ from each other in two amino acids (Ile80 in Capsid and Ala2611 in NS5 within Con1 ORF) (Supplementary Figure S3), Con1 grew significantly slower than PRVABC59 in Vero E6 and A549 cells over a 3-day culture period after infection with 0.01 MOI of each virus (Figure 1C). Similar growth attenuation was also observed at 3 dpi in the same cells after infection with a higher MOI (MOI of 0.1) (Supplementary Figures S4A and B).

Back mutations of the two amino acid changes present in the recombinant Con1 into the PRVABC59 reference (KU501215.1) sequences (namely Thr80 and Val2611) still rendered the resulting recombinant ZIKV Con1 (I80T/A2611V) less efficient than PRVABC59 (ATCC VR-1843; P2) in growth, in both Vero E6 and A549 cells (Figure 1D and E, and Supplementary Table S6).

The results prompted us to check genome sequences of PRVABC59 used in the infection experiments. We found, by sequencing analysis, that the P2 virus stock of PRVABC59 (passaged twice in Vero E6 cells after receiving the viral stock from ATCC) has subpopulations bearing five amino acid changes in envelope (E), NS1, and NS3 genes, compared to its reference sequence (Figure 1E) and Supplementary Table S7). The enhanced growth fitness of the PRVABC59 is thus likely due to heterogeneity of viral genome population in the PRVABC59 stock used in this study. Individual variants within these viral quasispecies might cooperate to increase the growth rate of PRVABC59 with a concomitant increase in its average plaque size (Figure 1F).

Effect of the 3'-end genome sequence variance between MR766 and Con1 on viral replication and translation

When determining a conserved ZIKV full-genome sequence, we had to choose one from two distinct viral 3'-end sequences found in Asian and African lineage ZIKV isolates. Analysis of full-genome

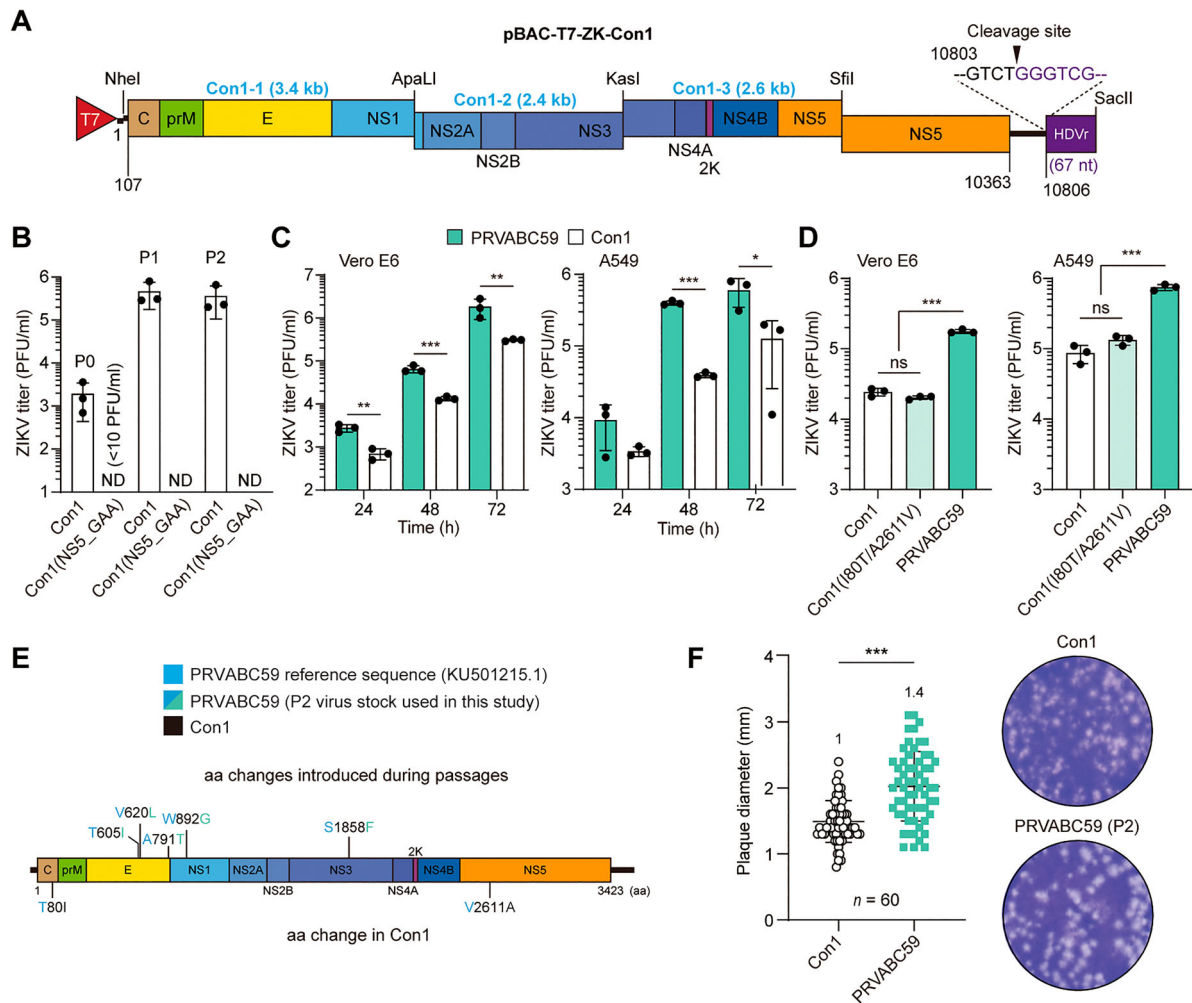


Figure 1. Construction of a full-length cDNA clone for a consensus sequence of ZIKV. (A) Schematic illustration of the full-length cDNA clone pBAC-T7-ZK-Con1, which harbours ZIKV cDNA fragments (Con1-1, Con1-2, and Con1-3 representing the ZIKV Con1 genome nt 37–3,445, 3,426–5,870, and 5,851–8,340, respectively) fused to T7 promoter and the cDNA of the last 2,392-nt (nt 8,416–10,806) of the Con1 sequence followed by HDV ribozyme (HDVr) and SacII restriction site. The four unique restriction enzyme sites used to assemble the cDNA fragments (Con1-1–3) into a modified pMW119 vector, prior to subcloning the resulting full-length cDNA into a BAC vector, are presented. (B) Infectivity of recombinant ZIKV Con1 rescued from Vero E6 cells transfected with T7 *in vitro* transcripts of pBAC-T7-ZK-Con1. Infectious viral titres of the Con1 viral stocks with indicated passage numbers were determined by plaque assay. Con1(NS5_GAA), a replication-defective mutant containing a GAA substitution at the active site of NS5 viral RdRp. ND, not detected (limit of detection, 10 PFU/ml). (C) Growth kinetics of PRVABC59 and Con1 in Vero E6 and A549 cells infected by each virus at an MOI of 0.01. (D) Growth attenuation features of Con1 and its derivative Con1(I80T/A2611V) in comparison with PRVABC59 strain in Vero E6 and A549 cells infected with each virus at an MOI of 0.01. (E) Differences in amino acid sequences between PRVABC59 reference sequence (GenBank KU501215.1), the PRVABC59 stock used in infection experiments in this study, and Con1. (F) Relative diameters of plaques from Con1 and the cell culture-adapted PRVABC59 ($n = 60$ plaques from 3 independent experiments). Plaque diameters were measured digitally using plaque images taken with the sizing bar. Right, representative images showing plaques 4 days after infection. In panels B–D, the results are the mean \pm SD from three independent replicates. Statistical analyses were performed using unpaired Student's *t*-test (C and F) or one-way ANOVA test (D) on \log_{10} -transformed data. * $P < 0.05$; ** $P < 0.01$; *** $P < 0.001$; ns, not significant.

sequences of ZIKV in the public databases revealed that the 3'-end sequence –UUUCU-3' detected in the East African strain MR766 is no longer found in Asian lineage ZIKV isolates and even in a West African isolate, DAK AR 41525 strain isolated in Senegal in 1984 (Figure 2A and Supplementary Table S8). The contemporary Asian lineage ZIKV has a conserved –GUCU-3' sequence, indicating that the UU at the 4–5 nt upstream of the 3'-end was evolutionarily changed to a single G residue in all Asian lineage ZIKV isolates.

It is currently unknown if this 3'-end sequence change introduced early in the course of ZIKV invasion into human populations had influenced on viral growth property and/or viral gene expression. To address this possibility, we first wanted to confirm that these two distinct 3'-end sequences are stably maintained in MR766 and PRVABC59 P2 stocks.

Using the viral genomic RNA prepared from culture media and the total RNA from infected cells, we constructed, by RACE-PCR, cDNA amplicons representing the 3'-end region (201-nt for MR766 and

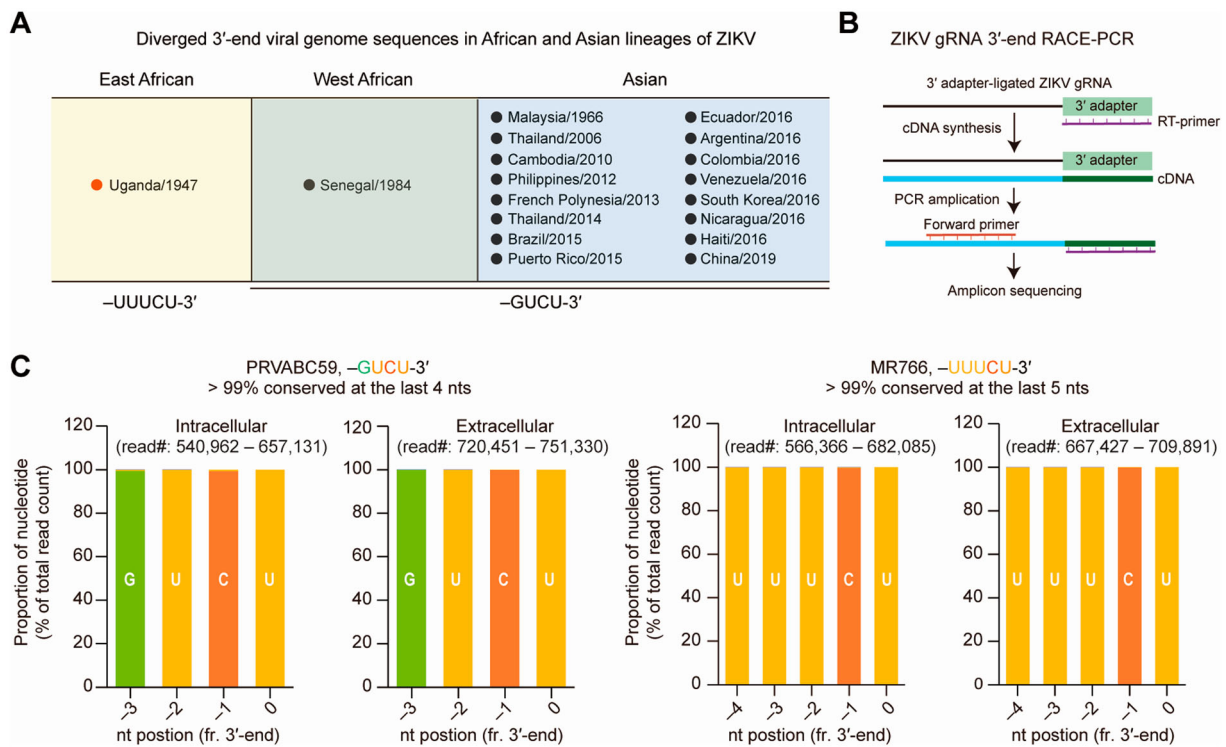


Figure 2. Conservation of the last 4-nt of ZIKV 3'-end genome sequence in contemporary Asian strains, diverged from the ancient African lineage MR766 strain. (A) Diverged 3'-end viral genome sequences in African and Asian lineage ZIKV isolates. (B and C) Schematic procedure of RACE-PCR. RNA was extracted from ZIKV MR766 strain (GenBank KX830960) and PRVABC59 (GenBank KU501215.1), ligated to the 5'-adenylated DNA adaptor, and reverse-transcribed to cDNA. The cDNA was amplified using a forward primer targeting the 3'-UTR of viral genome (nt 10,607–10,627) and a reverse primer targeting the 3'-adaptor (B). The amplicon libraries were sequenced on an Illumina Nextseq platform. Shown in (C) are the proportions of the last 4–5 nucleotides at the 3'-end of PRVABC59 and MR766 genomes.

200-nt for PRVABC59) of the genomes of these viruses (Figure 2B). The results of sequencing analysis showed that the lineage-specific terminal sequences are highly (> 99%) conserved, underscoring that this important *cis*-acting signal is stably inherited although the MR766 sequence appears to be evolved into the current –GUCU-3' end sequence now strictly conserved in contemporary Asian lineage ZIKV strains including PRVABC59 (Figure 2C).

We sought to address a question of why ZIKV was then evolved to alter its 3'-end sequences. We hypothesized that this terminal sequence divergence may have impact on viral replication and/or gene expression. To test this possibility, we constructed two subgenomic replicons derived from pBAC-CMV-ZK-Con1 that carry the authentic Con1 3'-end “–GTCT” and the East African lineage MR766 “–TTTCT” sequence alternatively (Figure 3A). The replicon expresses *Renilla* luciferase (Rluc), which was engineered to be processed from its precursor (Puro-2A-Rluc-2A) by the FMDV 2A autocleavage site [39]. This reporter-expressing ZIKV subgenomic replicon (Con1-sgRep) was sensitive to a broad-spectrum nucleoside analogue 2'-CMA, which was shown to display inhibitory activity against ZIKV [40] (Figure 3B). Using the verified replicon assay, we found that the replicon and its derivative with a

UUUCU substitution at the 3'-end [Con1_sgRep (UUUCU)] replicated to very similar levels (Figure 3C). As expected, Con1_sgRep(NS5_GAA) with a GAA substitution at the active site of NS5 RdRp failed to increase the reporter expression on day 2 above the baseline levels determined at 8 h post-transfection.

Further, viral gene expression was not affected upon replacing the –GUCU-3' at the 3'-UTR of a Con1 genome-derived Rluc-expressing ZIKV minigenome [Con1-minigenome-Rluc] with the –UUUCU-3' sequence (Figure 3D). Finally, an *in vitro* RNA decay assay using the Con1 FL 3'-UTR and its derivative with a UUUCU substitution revealed that their stability was not substantially altered by the 3'-terminal nucleotide change (–GUCU-3' to –UUUCU-3') (Figure 3E). Subgenomic flaviviral RNAs (sfRNAs) of various lengths (sfRNA1, sfRNA2, and sfRNA3), which are produced by the host 5'→3' exonuclease XRN1, are known to be critical for productive viral infection in both mammalian and mosquito cells [41]. The decay assay results also showed no difference in the kinetics of ZIKV-derived sfRNA accumulation. Furthermore, decay rate of the 3'-SL RNA was not influenced by these 3'-terminal sequences (Figure 3F). Similar results were also obtained with C6/36 mosquito cell lysates (Supplementary Figures S5).

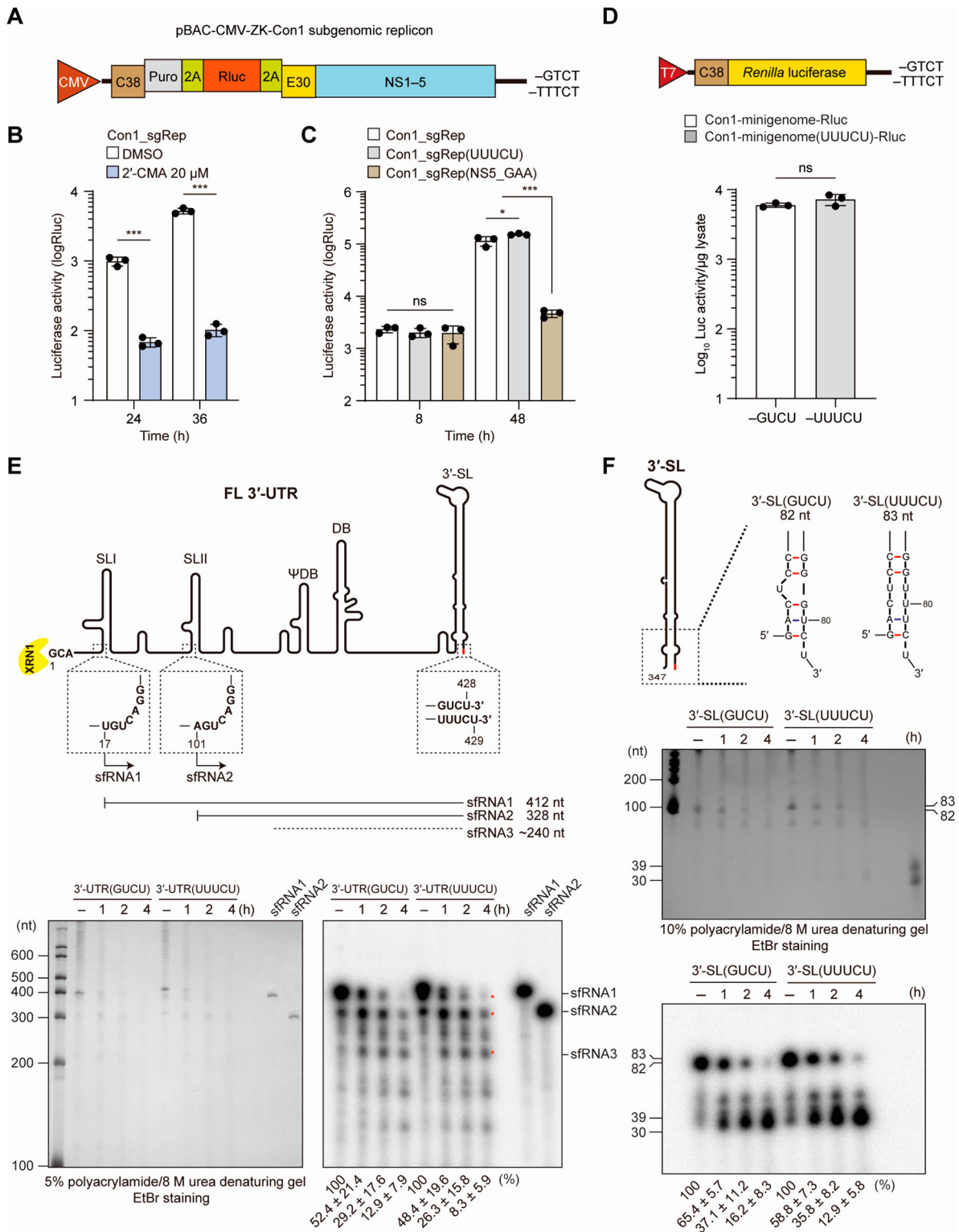


Figure 3. Effect of the ZIKV 3'-end sequence variance on viral replication and gene expression. (A) Schematic illustration of the pBAC-CMV-ZK-Con1 subgenomic replicon and its derivative terminating with a heterologous -TTTCT-3' end sequence originated from MR766. The puromycin resistance gene (Puro) and *Renilla* luciferase (Rluc) genes, which are separated from each other by FMDV 2A peptide-coding sequence, were in-frame fused downstream of the first 38 amino acids of the viral capsid gene (C38). (B) Inhibition of subgenomic replicon (Con1_sgRep) replication by 2'-C-methyladenosine (2'-CMA), an NS5 inhibitor. Rluc activity was measured at 24 and 36 h post-transfection of Huh7 cells with pBAC-CMV-ZK-Con1_sgRep. (C) Effect of the ZIKV 3'-end sequence variance on subgenomic replicon replication, assessed at the indicated time as described in (B). Con1_sgRep(NS5_GAA), a negative control expressing a defective NS5. (D) Effect of the ZIKV 3'-end sequence variations on viral RNA translation. Rluc activity was measured at 24 h post-transfection of Huh7 cells with the indicated Rluc-expressing *in vitro* transcribed ZIKV minigenomic RNAs where the Rluc gene was fused to the N-terminal part (38 amino acids) of capsid-coding gene placed in between viral 5'-UTR and 3'-UTR. (E and F) Schematic representation of the secondary structures of ZIKV FL 3'-UTR (E) and 3'-SL (F). SL, stem-loop; DB, dumbbell; sfRNA, subgenomic flavivirus RNA; XRN1, 5'→3' exoribonuclease 1. Decay kinetics of radioisotope-labeled *in vitro* transcripts of ZIKV FL 3'-UTR (E) and 3'-SL RNA (3'-SL) (F) with either -GUCU or -UUUCU 3'-terminal sequence in Vero E6 cell lysates (40 μg). The intensity of intact input RNA (mean ± SD from three independent experiments) quantified using a Phosphorimager was presented below representative autoradiography images. Statistical analyses were performed using unpaired Student's *t*-test (B and D) or one-way ANOVA test (C) on log₁₀-transformed data. **P* < 0.05; ****P* < 0.001; ns, not significant.

Altogether, our results provide evidence that the 3'-end viral genome sequence variation has little effect on viral replication and gene expression. Further, the 3'-end sequence variation did not alter decay rates of 3'-UTR or 3'-SL RNA, nor did it affect generation kinetics for sRNA species in Vero E6 and C6/36 cells.

The African and Asian lineage-specific 3'-end sequences are functionally equivalent in supporting viral propagation

In order to investigate whether the two distinct African and Asian lineage-specific 3'-end sequences are functionally equivalent in supporting viral propagation in the context of full-length viral genome, we constructed a pBAC-T7-ZK-Con1 derivative, pBAC-T7-ZK-Con1(TTTCT) where the 3'-end of Con1 was replaced by the MR766 3'-end sequence (-TTTCT-3'). The two recombinant viruses Con1 and Con1(UUUCU) replicated to similar levels on day 3 in Vero E6 and A549 cells (Figure 4A), suggesting that these two 3'-end sequences are compatible with the Con1-derived viral RNA replicase complex or NS5 RdRp.

We sought to further test whether a similar outcome can be also seen when the 3'-end of the prototype African strain MR766 is replaced by the Asian lineage counterpart, namely -GUCU-3'. To this end, we generated an infectious cDNA clone for MR766 strain (ATCC VR-84) using the viral RNA extracted from the P4 viral stock (passed 4 times in Vero E6) and its derivative bearing the Asian lineage-specific 3'-end sequence (Supplementary Figures S6A and B). The rescued recombinant rMR766 was infectious and, as shown in Supplementary Figure 6C, there was no significant difference in growth between rMR766 (P1) and its parental virus (P2 of MR766 ATCC VR-84). The MR766 infectious cDNA clone (GenBank ON123672) had four nt changes as compared with the MR766 reference sequence (KX830960.1), with 2 nonsynonymous mutations in NS3 and one dinucleotide change (UU→AG) within the 3'-UTR 3' stem-loop (3'-SL) region (Supplementary Figures 7A and B). Although these mutations did not affect viral growth, it remains to be studied whether the variant with these mutations outcompetes its parental virus during subsequent passages *in vitro* and if these variants generated via culture-adapted mutations or their mixtures can alter the virulence of MR766 *in vivo*.

Importantly, the two rescued recombinant viruses (P1), rMR766 and rMR766(GUCU) showed no discernible difference in viral loads at 3 dpi of Vero E6 and A549 cells (Figure 4B). Based on the results from experiments using recombinant Con1 and MR766 viruses with heterologous 3'-end sequence

substitutions, we concluded that the two evolutionally diverged ZIKV 3'-end sequences are equally compatible with African and Asian lineage ZIKVs in supporting their propagation *in vitro*.

African lineage ZIKV MR766 is equipped with a viral replicase complex more efficient than that of contemporary ZIKV

In the course of analysis of the potential evolutionary role of viral 3'-end sequence variations, we found that rMR766 grew faster than Con1 irrespective of the types of 3'-end sequence (Figures 4A and B). We wondered if this faster growth feature of MR766 was attributed to better replication competence of MR766 viral RNA replicase. To test the possibility, we constructed chimeric viruses between Con1 and rMR766 using their infectious cDNA clones (Figure 5A). The gene swapping experiments revealed that MR766 Nsp5 (NS1-NS5) in fact enabled the Con1 virus to gain increased replication capability, as evidenced by an increase in Con1/MR_NS1-5 viral loads. Notably, this replication enhancement effect could not be achieved by NS5 alone in the Con1/MR_NS5 chimeric virus (Figure 5B). In agreement with this, NS5 proteins of Con1 and rMR766 displayed similar *in vitro* RdRp activity in a primer-dependent poly(A)-copying assay, even though there are 34 amino acid differences (96.2% identity) between them (Supplementary Figure S8).

By contrast, rMR766 became less competent for replication when its Nsp5 were replaced by Con1 counterparts (rMR766 vs. rMR766/Con1_NS1-5) (Figure 5C). Taken together, these results demonstrate that MR766 is equipped with a more active viral replicase complex than Con1. Nevertheless, it should be noted that rMR766 viral load was significantly higher than that of the chimeric virus Con1/MR_NS1-5, suggesting that MR766 structural proteins also contribute to its better competence in propagation (Figure 5B). Supporting this possibility, a viral entry assay using Con1- and MR766-derived prME pseudotyped viruses revealed that the pseudotype MLV loaded with MR766 structural proteins was indeed superior to the one bearing Con1 prME in viral entry into host cells (Supplementary Figure S9).

Under the presumption that replication of African and Asian lineage ZIKVs can be influenced by the cellular protein milieu of mosquito cells, we compared growth kinetics of Con1 and its derivative expression MR766 NS1-5 (Con1/MR_NS1-5), along with rMR766 and its derivative expressing Con1_NS1-5 (rMR766/Con1_NS1-5) in C6/36 cells. The results showed that even in mosquito cells the African lineage MR766-derived Nsp5 (NS1-5) were capable of supporting ZIKV replication better than the counterparts of

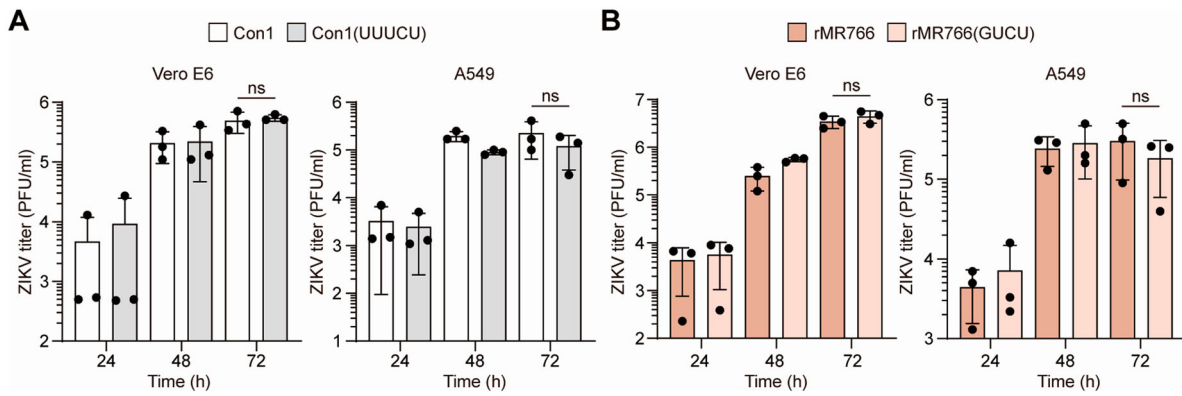


Figure 4. Functional equivalence of the evolutionally diverged ZIKV 3'-end sequences in viral genome replication. Comparisons of growth kinetics of Con1 (A) and rMR766 (B) with their derivatives Con1(UUUCU) and rMR766(GUCU) in Vero E6 and A549 cells (MOI = 0.01). ns, not significant (by unpaired Student's *t*-test).

Con1 (Supplementary Figure S10A). By contrast, the degree of viral titre difference between Con1 and rMR766 at 3 dpi was substantially reduced in this mosquito cell line than in Vero E6 (Supplementary Figure S10B). Strikingly, unlike what was observed in Vero E6 cells, Con1 and Con1/MR_NS1–5 replicated with a similar growth kinetics. The differences on viral amounts at 1, 2, and 3 dpi were not statistically apparent between Con1 and Con1/MR_NS1–5, whereas substitution of Con1_NS1–5 in rMR766 delayed its replication (Supplementary Figure S10A). Based the results from Vero E6 and C6/36 cells, we concluded that African-lineage ZIKV Nsp5 support viral replication more efficiently than the counterparts of Asian lineage ZIKV in both mammalian and mosquito cells.

ZIKV NS5 and Nsp5 (NS1–NS5) are virulence determinants in A129 mice

Having found that MR766 is more competent than the Con1 for replication *in vitro* and that its nonstructural

proteins (NS1–5), but not the viral RdRp NS5 alone, are required to confer this growth feature, we then hypothesized that the enhanced replication capacity of MR766 might be translated into virulence phenotype of this representative African lineage ZIKV strain. We tested the hypothesis by infecting the type I IFN-receptor-deficient A129 mice with a set of four recombinant ZIKV viruses, rMR766 and Con1 along with its two derivatives expressing MR766 NS5 (Con1/MR_NS5) or NS1–5 (Con1/MR_NS1–5) (Figure 6A). Weight loss in these infected mice was monitored over 15 days. On days 3 and 5, viral loads in sera ($n = 8$) were determined by plaque assays. On day 5, mice ($n = 6$) were sacrificed to determine viral RNA copy numbers in spleen, testis, kidney, brain, and liver tissues.

As shown in Figures 6B and C, rMR766 was highly virulent, leading to more than 20% weight loss in all of the infected mice ($n = 6$ with one female mouse dead) on day 7. Despite being delayed for 2 days, all mice infected with Con1/MR_NS1–5 also lost > 20% of

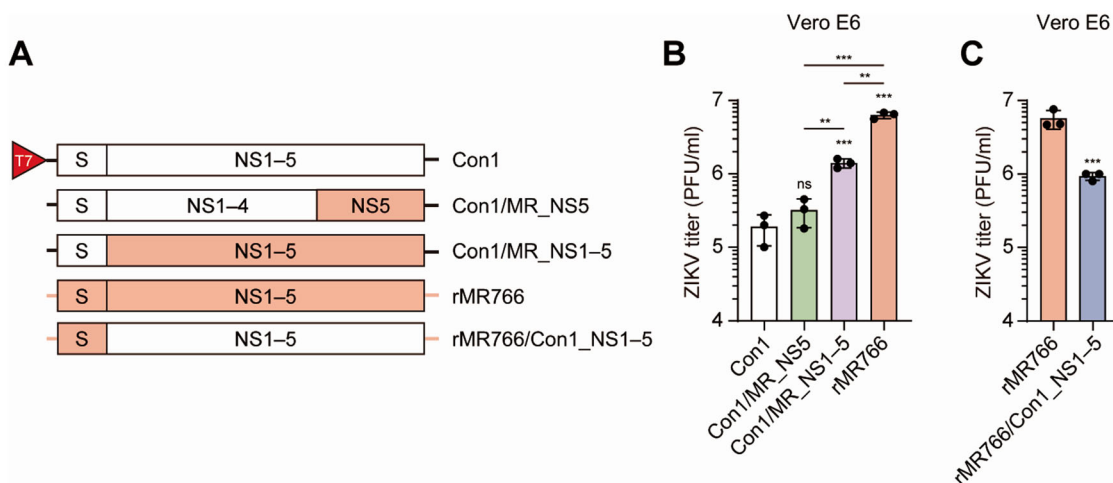


Figure 5. Growth kinetics of Con1, rMR766, and their chimaera expressing heterologous nonstructural viral proteins. (A) Schematics of ZIKV Con1 and MR766 chimeric viruses. (B and C) Growth kinetics of the indicated, rescued recombinant viruses in Vero E6 (MOI = 0.01, using P1 stock of each virus). Shown are the results (mean \pm SD) from three independent replicates. Statistical analyses were performed using one-way ANOVA test with multiple comparisons (B) or unpaired Student's *t*-test (C) on log₁₀-transformed data. ** $P < 0.01$; *** $P < 0.001$; ns, not significant.

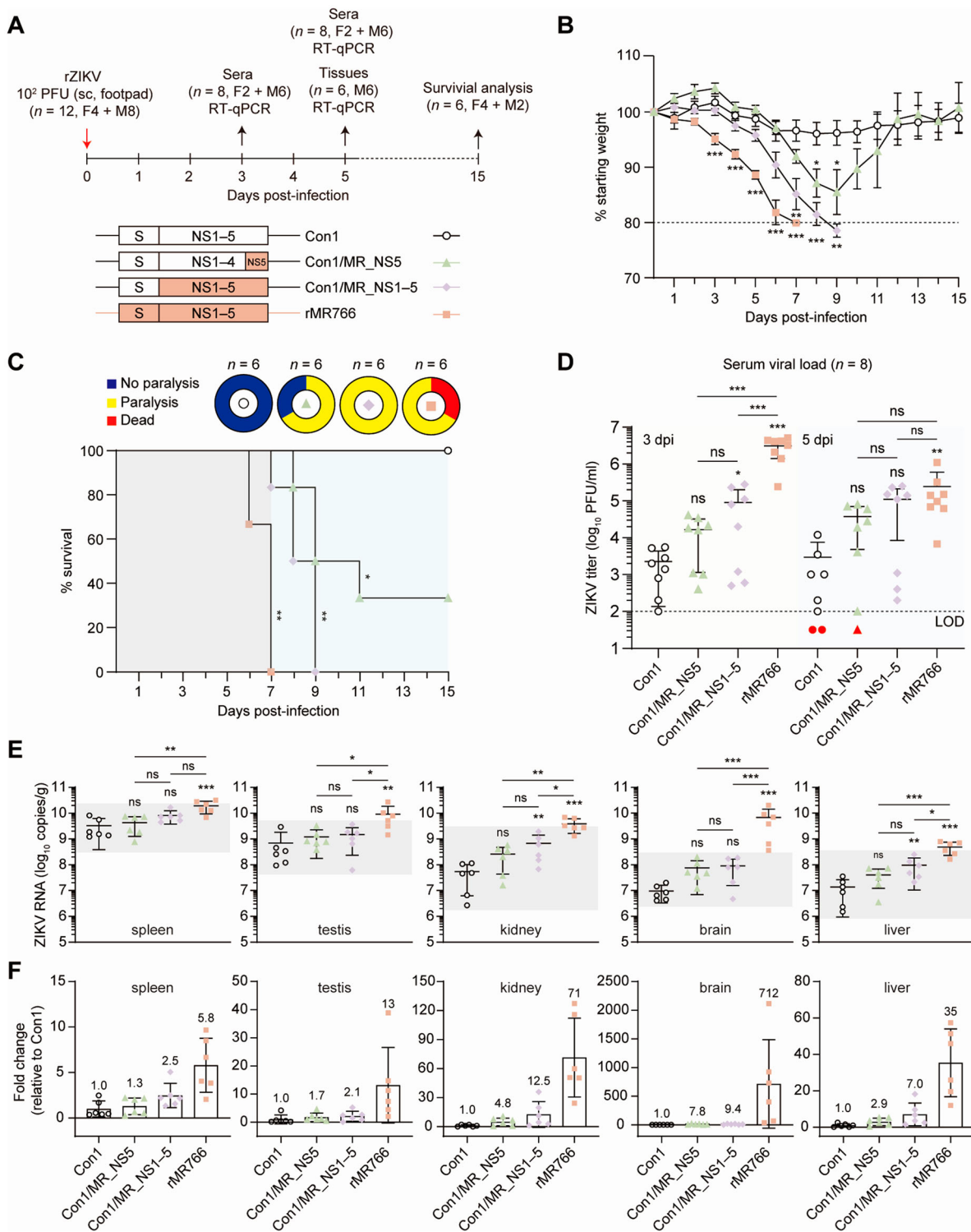


Figure 6. Virulence and neuropathogenicity of Con1 and Con1-derived chimeric viruses in A129 mice. (A) Infection and sample collection schedule (top). Schematics of chimeric viruses derived from Con1 and rMR766 (bottom). (B and C) For survival analysis, IFNAR^{-/-} A129 mice ($n = 12$ with 4 female and 8 male) were infected with each ZIKV (10^2 PFU) by sc injection into the footpad. Body weight was monitored daily for 15 days (B). Combined data from two independent experiments are shown as mean \pm SEM. Comparisons of Kaplan-Meier survival curves between different groups were performed by log-rank analysis (C). Shown in doughnut charts is the frequency of paralysis observed in infected mice. (D–F) Viral loads in sera on days 3 and 5 (D) and in indicated tissues on day 5 (E). The dotted lines in (D) shows the limit of detection (LOD). Shown in (F) are fold-changes in viral genome copy number in tissues with mean values indicated at the top of each bar. Each dot represents a result from a separate animal. Statistical analyses were performed using unpaired Student's *t*-test (B) or one-way ANOVA test with multiple comparisons on log₁₀-transformed data (D and E). * $P < 0.05$; ** $P < 0.01$; *** $P < 0.001$; ns, not significant.

their initial body weight on day 9, with all displaying bilateral hind limb paralysis starting on day 7. Two out of six of Con1/MR_NS5-infected mice survived

15 days, while the mice with $> 20\%$ weight loss exhibited staggered steps and hind-leg paralysis starting on day 8.

The serum viral loads for rMR766 viral loads were $\sim 10^6$ PFU/ml on day 3, followed by a decline to 2.4×10^5 PFU/ml on day 5, while mean values of viral loads for Con1, Con1/MR_NS5, and Con1/MR_NS1-5 were less than 10^5 PFU/ml on days 3 and 5 (Figure 6D). In mice ($n = 6$) sacrificed on day 5, rMR766 viral RNA levels in all examined tissues, except spleen, were higher than those of Con1, Con1/MR_NS5, Con1/MR_NS1-5 (Figure 6E). Notably, viral RNA copy number of rMR766 was 712-fold higher in brain than that of Con1 (Figure 6F). Higher titres of rMR766 viruses in brain as well as in other organs explain the differences in virulence between this African lineage of ZIKV and the Con1.

Similarly, both paralysis and mortality rate increased in mice exposed to Con1/MR_NS5 or Con1/MR_NS1-5, although a statistically significant difference in serum viral loads was only observed between Con1 and Con1/MR_NS1-5 at 3 dpi. At 5 dpi, the difference became marginal although a significant difference in viral RNA levels was still observed in kidney and liver tissues. Collectively, the results imply that the virulence enhancement caused by MR766 NS1-5 in the Con1 chimaera (Con1/MR766 NS1-5) appears to be associated with its replication competence, while MR766 NS5 alone was not sufficient to explain the striking correlation between MR766 Nsp's replication competence and virulence.

Replication competence and virulence of rZIKVs in wild-type C57BL/6 mice transiently blocked in type I IFN signaling

We further investigated the potential impact of ZIKV Nsps on brain pathogenesis in C57BL/6 mice ($n = 10$) transiently blocked in IFN signaling pathway by injecting (ip) an anti-type I IFN receptor (IFNAR1) antibody MAb-5A3 [42]. The clinical performance and body weight of the infected mice were monitored daily for 15 days (Figure 7A). We collected sera at different time points post-infection (4 and 7 dpi), and sacrificed the mice (five male mice to determine viral RNA levels in testes) at 7 dpi to determine viral loads in sera and tissues and to analyze the pathological changes in the brain. As shown in Figures 7B–D, around 60% of mice exposed to rMR766 died on day 7, accompanied by a gradual hindlimb weakness progressed to complete paralysis with a complete mortality rate (100%) by day 8. These recapitulate the severe symptoms caused by rMR766, as also observed in A129 mice.

In contrast to the results observed in A129 mice, the mice exposed to Con1 or even its two derivatives expressing MR766 Nsps (Con1/MR_NS5 and Con1/MR_NS1-5) survived with no clinical signs of distress, such as shaking/shivering or limb paralysis during the

course of experiment (Figure 7D). A significant body weight loss, only observed on days 7 and 8 post-infection of the mice exposed to Con1/MR_NS1-5, slowly started to be normalized by day 15. Likewise, we observed no significant decreases in body weight in the mice exposed to Con1/MR_NS5.

Despite there being no discernible difference in virulence among Con1 and its two derivatives Con1/MR_NS5 and Con1/MR_NS1-5, a substantial difference in growth rate between Con1/MR_NS5 (more dramatically with Con1) and Con1/MR_NS1-5 was observed in the WT C57BL/6 mice treated with MAb-5A3 antibody (Figures 7E–G)). In this mouse infection model mimicking a partial type I IFN signaling blocking state caused by ZIKV NS5-mediated human, but not mouse, STAT2 degradation [43], Con1 replication, as observed in Vero cells known to be defective in IFN production [44,45], was enhanced by MR766 NS1-5 and even by NS5 alone, as evidenced by increased viral loads (RNA genome and infectious virus levels) on 4 and 7 dpi.

However, differing from the results from A129 mice, Con1/MR_NS1-5 infection caused no death of the mice by day 8, although its RNA levels in all analyzed tissues (except for kidney) were comparable to those of rMR766 by up to day 7 post-infection (Figures 7H and I). Histopathological analysis with H&E staining of cerebral cortex showed dense perivascular cuffs of lymphocytes and necrotic loci in rMR766-infected mice (Figure 7J). Con1-MR_NS1-5 infection was also characterized by a perivascular cuff of inflammatory cells at day 7 post-infection. Altogether, our results suggest that the MR766 Nsps, which are capable of enhancing Con1 replication, and its structural proteins, which we showed to be more effective than the Con1 counterparts in viral entry into host cells (Supplementary Figure S9) contribute together to the full virulence of the highly pathogenic African lineage ZIKV MR766, with the former ones displaying their virulence phenotypes more substantially in immunocompromised hosts.

Discussion

The data presented here provide insights into evolution of ZIKV 3'-terminal sequences and virally encoded Nsps including NS5 RdRp. We found that the 3'-end viral genome sequence –GUCU-3', which is conserved in currently prevailing Asian ZIKV strains, is functionally equivalent to the –UUUCU-3' sequence of the prototype African strain MR766 identified over 70 years ago. Our results also reveal an unprecedented role of ZIKV Nsps in determining ZIKV virulence. Based on our findings, we propose that the genetic drifts within the Nsps or NS5, which have been introduced in large numbers during African lineage ZIKV evolution, may alter

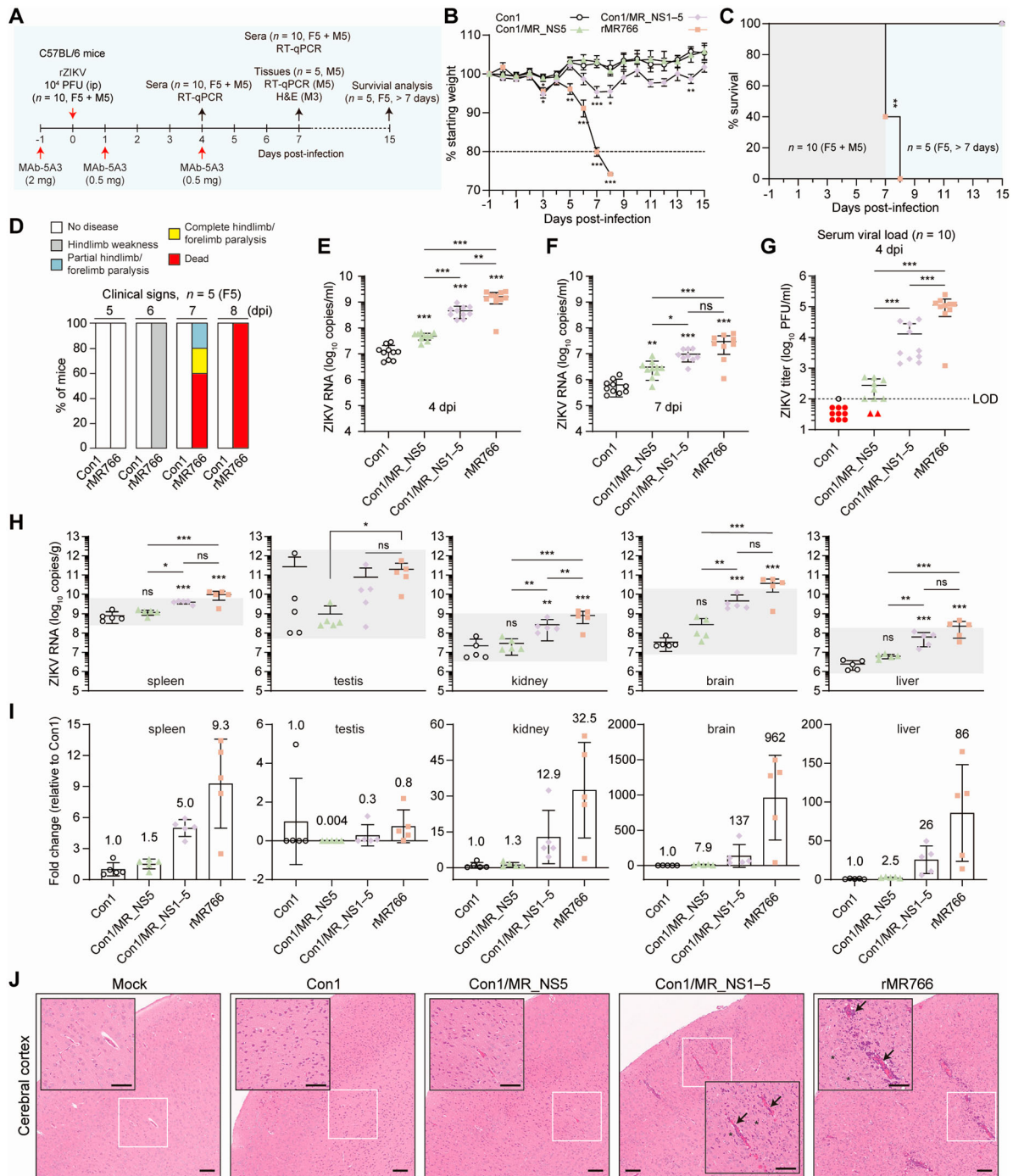


Figure 7. African lineage ZIKV structural proteins account for the enhanced pathogenicity of MR766 in wild-type C57BL/6 mice transiently blocked in type I IFN signaling. (A) Schematic of experimental design showing the infection, antibody injection, and sample collection schedule. (B and C) Body weight changes and survival analysis of C57BL/6 mice (six-week-old, $n = 10$ per each group with 5 female and 5 male mice) treated with an anti-type I IFN antibody MAb-5A before and after being exposed to 10^4 PFU (ip injection) of indicated rZIKVs. Statistical analysis methods are identical to those described in Figures 6B and C. (D) Clinical disease in mice infected with indicated rZIKVs on different days of post-infection. Bar charts show the frequency of five different clinical signs of disease. (E–I) Comparison of viral RNA levels (E, F, H, and I) or infectious viral loads (G) in sera (E, F, and G) and tissues (H and I) between mice on 4 and 7 dpi with indicated rZIKVs. Each dot represents a result from a separate animal. (J) Brain tissue samples of infected mice were collected on 7 dpi, stained with H&E for histopathological evaluation. Representative micrographs of the cortex of mock- and rZIKV-infected mice, with higher magnification images (inset) of the area outlined by the white box. Arrows, perivascular cuffing with infiltration of inflammatory cells in the brain tissues (cerebral cortex) of infected mice; asterisk, necrotic cellular debris. Scale bars, 100 μm . In (E–H), statistical analyses were performed using one-way ANOVA test with multiple comparisons on log₁₀-transformed data. * $P < 0.05$; ** $P < 0.01$; *** $P < 0.001$; ns, not significant.

interplays between these proteins and host factors, resulting in virulence attenuation in contemporary ZIKV strains.

Our results show that the G and UU sequences 4 nt upstream of the 3'-end of viral genome are interchangeable between African and Asian lineage ZIKVs. It is not

clear when the UU → G change was introduced during ZIKV evolution, due to the very limited number of complete genome sequences of African lineage ZIKV strains. However, by gene swapping experiments using infectious cDNA clones for MR766 and Con1, we demonstrate that both African (MR766) and Asian (Con1) lineage ZIKV are compatible with the two different 3'-end sequences, namely -UUUCU-3' and -GUCU-3'. The data are consistent with previous studies on multiple infectious cDNA clones for African and Asian lineage ZIKV isolates [23,31,46–55]. All the clones of MR766 constructed previously had the -UUUCU-3' terminal sequence [46–48], while the other clones for Asian or American isolates included the -GUCU-3' sequence [23,31,47,49–55]. Interestingly, DAK AR 41525 strain isolated in Senegal in 1984, which has an Asian lineage-specific terminal sequence -GUCU-3', could be rescued from a cDNA clone bearing this 3'-terminal sequence [23]. The results from these previous studies suggested the potential compatibility of these sequences in both ancient and contemporary ZIKVs. In agreement with this, our results provide direct evidence that these two distinct sequences are functionally equivalent in the context of full-length genomes of African and Asian lineage ZIKVs. We did not observe obvious differences in viral replication and gene expression between the two Con1 (or MR766) viruses with -GUCU-3' or -UUUCU-3' terminal sequence.

Although it is currently unclear if there are any beneficial outcomes of this UU → G change during ZIKV evolution, we observed conservation of these sequence variations in both MR766 and PRVABC59 strains. Flaviviruses have a unique 3'-end sequence terminating with a conserved CU_{OH} instead of a poly(A) tract. Reverse genetics studies revealed that the 3'-terminal dinucleotides CU_{OH} are critical residues that cannot be replaced by other nonconserved sequences in various flaviviruses such as Kunjin virus and dengue virus [26,27]. Our RNA sequencing results confirmed that the 3'-terminal dinucleotides CU is maintained stably during ZIKV evolution and passages. Of note, although the -GUCU-3' and -UUUCU-3' sequences are functionally interchangeable, there was no emergence of variants with any mutations on these terminal sequences. Taken together, our results posit that the last 4–5 nt conserved sequences at the 3'-SL of ZIKV 3'-UTR are critical *cis*-acting RNA element needed to be stably inherited for viral replication.

Although severe disease manifestation in human cases had not been reported for African lineage ZIKV, it was shown to be more virulent than Asian lineage ZIKV in mouse infection models as well as *in vitro* [21–24,34]. The degrees of ZIKV virulence would be influenced by genetic variances between these two lineages that can alter their

replication competence and/or functions of viral gene products in addition to the outcomes of interplays between mutated viral proteins and their cellular targets [41]. African and Asian strains differ from each other by approximately 3.5% at the amino acid level [56]. Flavivirus structural proteins are primarily engaged in binding, entry, and assembly of virus particles. ZIKV structural proteins (capsid, prM, and E) were suggested to account for the virulence of African lineage ZIKV in an IFN- α/β receptor knockout mouse model [23,24]. Nakayama *et al.* [24] reported that the lethality of MR766 in the IFNAR^{-/-} mice was attributed to its prM protein with increased ability to cross the blood–brain barrier [24]. Expanding on these earlier reports, our results show that nonstructural proteins are additional critical factors of virulence and neurological symptoms displayed by MR766, particularly in immunocompromised hosts.

Such virulence phenotypes including limb paralysis with high mortality risk were not seen in mice exposed to Con1. In A129 mice, rMR766 were more pathogenic (100% mortality) than Con1 strain (100% survival). Importantly, substitution of Con1 Nsp genes with MR766 counterparts dramatically increased morbidity and mortality of the resulting chimaera of Con1. These results suggest that the attenuated virulence of Con1 can be attributed to multiple adaptive mutations in nonstructural proteins. Further, even MR766 NS5 alone increased the chance of hind limb paralysis and mortality of Con1. There are 77 amino acid differences in Nsps between Con1 and MR766 (Supplementary Figure S11). Thus, one may envision that these amino acid differences might account for the severe paralysis and mortality associated with MR766 NS5 or NS1–5. Of the 7 different Nsps, NS5 showed the greatest level of genetic drift. Despite there being 34 amino acid differences between MR766 and Con1 strains, their NS5 proteins showed a similar RdRp activity *in vitro* (Supplementary Figure S8E).

In A129 mice, viral amounts produced by Con1 and Con1/MR_NS5 were not significantly different from each other. In C57BL/6 mice transiently blocked in type I IFN signaling, the difference in viral RNA levels in tissues between these two rZIKVs were negligible, despite there being a significant difference in sera. Notably, in the C57BL/6 mice pretreated with an IFNAR1 antibody, Con1/MR_NS5 infection did not cause paralysis. In addition, no lymphocyte infiltration was evident in the brain of infected mice. The lack of the severe clinical signs in this partially immunocompromised mouse suggests that the serious symptoms developed upon infection with Con1/MR_NS5 in the IFNAR^{-/-} mice might not be associated with increased viral loads or not be strictly dependent on replicating competence of the NS5 RdRp. Similar

attenuated symptoms were also observed for Con1/MR_NS1–5 in the IFNAR1 antibody-pretreated C57BL/6 mice. Therefore, the virulence directed by African a lineage ZIKV NS5 or Nsp5 (NS1–5) could be the outcome of dysregulated interplays of these Nsp5 with host cells in type I IFN signaling-compromised states.

Besides their roles in viral RNA replication, ZIKV Nsp5 (NS1, NS2A, NS2B, NS3, NS4A, NS4B, and NS5) are used to evade host immune responses via various mechanisms. The NS1, NS2A, NS2B, and NS4B of ZIKV inhibit phosphorylation of TANK-binding kinase I (TBK1), NS2B inhibit phosphorylation of IRF3, NS2B interferes with JAK/STAT signaling pathway by promoting JAK1 degradation, and NS5 antagonizes type I IFN signaling by degrading human, but not mouse, STAT2, and suppresses the IFN signaling at a downstream step of IRF3 phosphorylation [43,57,58]. In addition to these multifunctional roles of NS5, with its primary role in virus RNA replication taking place in the cytoplasm, presence of ZIKV NS5 in unique spherical shell-like structures within the nuclei of infected cells [59] suggest as-yet-unidentified regulatory functions of NS5 in the nucleus. The results from C57BL/6 and A129 mice demonstrate that the degree of virulence promoted by the MR766 Nsp5 can be influenced by host type I IFN signaling. Further studies are needed to understand the underlying mechanisms behind the virulence conferred by NS5 as well as the rest of the Nsp5.

Conclusions

In conclusion, we propose a hypothesis of functionally compatible evolution of the Asian lineage ZIKV 3'-end sequence –GUCU-3' diverged from the African lineage ZIKV 3'-terminal sequence –UUUCU-3'. Our reverse genetics-based studies define the role of viral Nsp-coding genes in determining ZIKV virulence. The results of this study suggest that the genetic drifts accumulated within ZIKV Nsp5 during evolution account for the attenuated virulence features of currently circulating Asian strains of ZIKV, identifying an additional mechanism besides the previously disclosed prM-mediated virulence trait of MR766. Moreover, we show for the first time that viral RdRp NS5 of MR766 is a virulence factor that increases the risk of paralysis and mortality in mice defective in type I IFN signaling. Our findings uncover an unprecedented role of ZIKV Nsp5 in determining viral pathogenicity in immunocompromised hosts. Identification of a critical determinant of ZIKV neuropathogenesis and elucidation of its impact in individuals defective in the interferon signaling pathway and immunocompromised hosts will provide insights into how neurotropic flaviviruses cause profound and life-long neurological defects.

Disclosure statement

J.-W.O., H.-G.J, and H.C. are inventors on a pending patent related to this work filed by University Industry Foundation (UIF), Yonsei University. The remaining authors have no conflicts of interest to declare.

Funding

This work was supported by the Korea Health Technology R&D Project grant (HI20C0010) through the Korea Health Industry Development Institute (KHIDI), funded by the Ministry of Health & Welfare, Korea, and in part by the National Research Foundation of Korea (NRF) grants (2020R1A2C2005170 and 2022M3E5F1016361) funded by the Ministry of Science and ICT (MIST), South Korea. Open access publication fee was supported by the Brain Korea 21 (BK21) FOUR program. H.C. was in part supported by a postdoctoral fellowship from the Brain Korea 21 (BK21) FOUR program.

ORCID

Seong-Jun Kim  <http://orcid.org/0000-0001-8504-2872>
Jong-Won Oh  <http://orcid.org/0000-0001-8851-234X>

References

- [1] Oehler E, Watrin L, Larre P, et al. Zika virus infection complicated by Guillain-Barre syndrome - case report, French Polynesia, December 2013. *Euro Surveill.* 2014;19(9):4–6.
- [2] Fauci AS, Morens DM. Zika virus in the Americas - yet another Arbovirus threat. *N Engl J Med.* 2016;374(7):601–604.
- [3] Dick GWA, Haddock AJ, Uganda S. Virus. A hitherto unrecorded virus isolated from mosquitoes in Uganda. (I). Isolation and pathogenicity. *Trans R Soc Trop Med Hyg.* 1952;46(6):600–618.
- [4] Boorman JP, Draper CC. Isolations of arboviruses in the Lagos area of Nigeria, and a survey of antibodies to them in man and animals. *Trans R Soc Trop Med Hyg.* 1968;62(2):269–277.
- [5] Wikan N, Smith DR. First published report of Zika virus infection in people: Simpson, not MacNamara. *Lancet Infect Dis.* 2017;17(1):15–17.
- [6] Simpson DI. Zika virus infection in man. *Trans R Soc Trop Med Hyg.* 1964;58:335–338.
- [7] MacNamara FN. Zika virus: a report on three cases of human infection during an epidemic of jaundice in Nigeria. *Trans R Soc Trop Med Hyg.* 1954;48(2):139–145.
- [8] Marchette NJ, Garcia R, Rudnick A. Isolation of Zika virus from *Aedes aegypti* mosquitoes in Malaysia. *Am J Trop Med Hyg.* 1969;18(3):411–415.
- [9] Olson JG, Ksiazek TG, Suhandiman, et al. Zika virus, a cause of fever in Central Java, Indonesia. *Trans R Soc Trop Med Hyg.* 1981;75(3):389–393.
- [10] Chan JFW, Choi GKY, Yip CCY, et al. Zika fever and congenital Zika syndrome: an unexpected emerging arboviral disease. *J Infection.* 2016;72(5):507–524.
- [11] Duffy MR, Chen TH, Hancock WT, et al. Zika virus outbreak on Yap Island, Federated States of Micronesia. *N Engl J Med.* 2009;360(24):2536–2543.

- [12] Musso D. Zika virus transmission from French Polynesia to Brazil. *Emerg Infect Dis.* 2015;21(10):1887.
- [13] Cao-Lormeau VM, Roche C, Teissier A, et al. Zika virus, French Polynesia, South Pacific, 2013. *Emerg Infect Dis.* 2014;20(6):1085–1086.
- [14] Teixeira MG, Costa MDN, de Oliveira WK, et al. The epidemic of Zika virus-related microcephaly in Brazil: detection, control, etiology, and future scenarios. *Am J Public Health.* 2016;106(4):601–605.
- [15] Wang L, Valderramos SG, Wu AP, et al. From mosquitoes to humans: genetic evolution of Zika virus. *Cell Host Microbe.* 2016;19(5):561–565.
- [16] Rusanov T, Kent T, Saeed M, et al. Identification of a small interface between the methyltransferase and RNA polymerase of NS5 that is essential for Zika virus replication. *Sci Rep.* 2018;8(1):17384.
- [17] Kim Y-G, Yoo J-S, Kim J-H, et al. Biochemical characterization of a recombinant Japanese encephalitis virus RNA-dependent RNA polymerase. *BMC Mol Biol.* 2007;8(1):59.
- [18] Pettersson JHO, Eldholm V, Seligman SJ, et al. How did Zika virus emerge in the Pacific Islands and Latin America? *mBio.* 2016;7(5):e01239–16.
- [19] Marzi A, Emanuel J, Callison J, et al. Lethal Zika virus disease models in young and older interferon alpha/beta receptor knock out mice. *Front Cell Infect Microbiol.* 2018;8:117.
- [20] Anfasa F, Siegers JY, van der Kroeg M, et al. Phenotypic differences between Asian and African lineage Zika viruses in human neural progenitor cells. *mSphere.* 2017;2(4):e00292–17.
- [21] Dowall SD, Graham VA, Rayner E, et al. Lineage-dependent differences in the disease progression of Zika virus infection in type-I interferon receptor knockout (A129) mice. *PLoS Negl Trop Dis.* 2017;11(7):e0005704.
- [22] Duggal NK, Ritter JM, McDonald EM, et al. Differential neurovirulence of African and Asian genotype Zika virus isolates in outbred immunocompetent mice. *Am J Trop Med Hyg.* 2017;97(5):1410–1417.
- [23] Nunes BTD, Fontes-Garfias CR, Shan C, et al. Zika structural genes determine the virulence of African and Asian lineages. *Emerg Microbes Infect.* 2020;9(1):1023–1033.
- [24] Nakayama E, Kato F, Tajima S, et al. Neuroinvasiveness of the MR766 strain of Zika virus in IFNAR^{-/-} mice maps to prM residues conserved amongst African genotype viruses. *PLoS Pathog.* 2021;17(7):e1009788.
- [25] Yuan L, Huang XY, Liu ZY, et al. A single mutation in the prM protein of Zika virus contributes to fetal microcephaly. *Science.* 2017;358(6365):933–936.
- [26] Nomaguchi M, Ackermann M, Yon CS, et al. *De novo* synthesis of negative-strand RNA by dengue virus RNA-dependent RNA polymerase *in vitro*: nucleotide, primer, and template parameters. *J Virol.* 2003;77(19):8831–8842.
- [27] Khromykh AA, Kondratieva N, Sgro JY, et al. Significance in replication of the terminal nucleotides of the *Flavivirus* genome. *J Virol.* 2003;77(19):10623–10629.
- [28] Schurer H, Lang K, Schuster J, et al. A universal method to produce *in vitro* transcripts with homogeneous 3' ends. *Nucleic Acids Res.* 2002;30(12):e56.
- [29] Ahn DG, Lee W, Choi JK, et al. Interference of ribosomal frameshifting by antisense peptide nucleic acids suppresses SARS coronavirus replication. *Antiviral Res.* 2011;91(1):1–10.
- [30] Li JQ, Deng CL, Gu DY, et al. Development of a replicon cell line-based high throughput antiviral assay for screening inhibitors of Zika virus. *Antiviral Res.* 2018;150:148–54.
- [31] Tsetsarkin KA, Kenney H, Chen RB, et al. A full-length infectious cDNA clone of Zika virus from the 2015 epidemic in Brazil as a genetic platform for studies of virus-host interactions and vaccine development. *mBio.* 2016;7(4):e01114–16.
- [32] Baer A, Kehn-Hall K. Viral concentration determination through plaque assays: using traditional and novel overlay systems. *J Vis Exp.* 2014;93:e52065.
- [33] Sardi Silvia I, Somasekar S, Naccache Samia N, et al. Coinfections of Zika and Chikungunya viruses in Bahia, Brazil, identified by metagenomic next-generation sequencing. *J Clin Microbiol.* 2016;54(9):2348–2353.
- [34] Aubry F, Jacobs S, Darmuzey M, et al. Recent African strains of Zika virus display higher transmissibility and fetal pathogenicity than Asian strains. *Nat Commun.* 2021;12(1):916.
- [35] Kim M, Cho H, Ahn D-G, et al. *In vitro* replication inhibitory activity of xanthorrhizol against severe acute respiratory syndrome coronavirus 2. *Biomedicines.* 2021;9(11):1725.
- [36] Cho H, Lee W, Kim GW, et al. Regulation of La/SSB-dependent viral gene expression by pre-tRNA 3' trailer-derived tRNA fragments. *Nucleic Acids Res.* 2019;47(18):9888–9901.
- [37] Li H, Durbin R. Fast and accurate long-read alignment with Burrows-Wheeler transform. *Bioinformatics.* 2010;26(5):589–595.
- [38] Rana J, Campos JLS, Leccese G, et al. Role of capsid anchor in the morphogenesis of Zika virus. *J Virol.* 2018;92(22):e01174–18.
- [39] Xie X, Zou J, Shan C, et al. Zika virus replicons for drug discovery. *EBioMedicine.* 2016;12:156–160.
- [40] Eyer L, Nencka R, Huvarová I, et al. Nucleoside inhibitors of Zika virus. *J Infect Dis.* 2016;214(5):707–711.
- [41] Pallarés HM, Navarro GSC, Villordo SM, et al. Zika virus subgenomic *Flavivirus* RNA generation requires cooperativity between duplicated RNA structures that are essential for productive infection in human cells. *J Virol.* 2020;94(18):e00343–20.
- [42] Sheehan KCF, Lai KS, Dunn GP, et al. Blocking monoclonal antibodies specific for mouse IFN-alpha/beta receptor subunit 1 (IFNAR-1) from mice immunized by *in vivo* hydrodynamic transfection. *J Interf Cytok Res.* 2006;26(11):804–819.
- [43] Grant A, Ponia SS, Tripathi S, et al. Zika virus targets human STAT2 to inhibit type I interferon signaling. *Cell Host Microbe.* 2016;19(6):882–890.
- [44] Emery JM, Morgan MJ. Regulation of the interferon system: evidence that Vero cells have a genetic defect in interferon production. *J Gen Virol.* 1979;43(1):247–252.
- [45] Kim M, Cho H, Lee SH, et al. An infectious cDNA clone of a growth attenuated Korean isolate of MERS coronavirus KNIH002 in clade B. *Emerg Microbes Infect.* 2020;9(1):2714–2726.
- [46] Gadea G, Bos S, Krejbich-Trotot P, et al. A robust method for the rapid generation of recombinant Zika virus expressing the GFP reporter gene. *Virology.* 2016;497:157–162.

- [47] Munster M, Plaszczynca A, Cortese M, et al. A reverse genetics system for Zika virus based on a simple molecular cloning strategy. *Viruses*. 2018;10(7):368.
- [48] Schwarz MC, Sourisseau M, Espino MM, et al. Rescue of the 1947 Zika virus prototype strain with a cytomegalovirus promoter-driven cDNA clone. *mSphere*. 2016;1(5):e00246–16.
- [49] Shan C, Xie XP, Muruato AE, et al. An infectious cDNA clone of Zika virus to study viral virulence, mosquito transmission, and antiviral inhibitors. *Cell Host Microbe*. 2016;19(6):891–900.
- [50] Yang YJ, Shan C, Zou J, et al. A cDNA clone-launched platform for high-yield production of inactivated Zika vaccine. *EBioMedicine*. 2017;17:145–156.
- [51] Weger-Lucarelli J, Duggal NK, Bullard-Feibelman K, et al. Development and characterization of recombinant virus generated from a new world Zika virus infectious clone. *J Virol*. 2017;91(1):e01765–16.
- [52] Marquez-Jurado S, Nogales A, Avila-Perez G, et al. An alanine-to-valine substitution in the residue 175 of Zika virus NS2A protein affects viral RNA synthesis and attenuates the virus in vivo. *Viruses*. 2018;10(10):547.
- [53] Avila-Perez G, Nogales A, Park JG, et al. A natural polymorphism in Zika virus NS2A protein responsible of virulence in mice. *Sci Rep*. 2019;9(1):19968.
- [54] Deng CL, Zhang QY, Chen DD, et al. Recovery of the Zika virus through an *in vitro* ligation approach. *J Gen Virol*. 2017;98(7):1739–1743.
- [55] Chen Y, Liu T, Zhang Z, et al. Novel genetically stable infectious clone for a Zika virus clinical isolate and identification of RNA elements essential for virus production. *Virus Res*. 2018;257:14–24.
- [56] Willard KA, Demakovsky L, Tesla B, et al. Zika virus exhibits lineage-specific phenotypes in cell culture, in *Aedes aegypti* mosquitoes, and in an embryo model. *Viruses*. 2017;9(12):383.
- [57] Wu YX, Liu QX, Zhou J, et al. Zika virus evades interferon-mediated antiviral response through the cooperation of multiple nonstructural proteins *in vitro*. *Cell Discov*. 2017;3:17006.
- [58] Xia HJ, Luo HL, Shan C, et al. An evolutionary NS1 mutation enhances Zika virus evasion of host interferon induction. *Nat Commun*. 2018;9(1):414.
- [59] Tan MJA, Chan KWK, Ng IHW, et al. The potential role of the ZIKV NS5 nuclear spherical-shell structures in cell type-specific host immune modulation during ZIKV infection. *Cells-Basel*. 2019;8(12):1519.